

Fast detection of genetic information by an optimized PCR in an interchangeable chip

Jinbo Wu · Rimantas Kodzius · Kang Xiao ·
Jianhua Qin · Weijia Wen

Published online: 6 October 2011
© Springer Science+Business Media, LLC 2011

Abstract In this paper, we report the construction of a polymerase chain reaction (PCR) device for fast amplification and detection of DNA. This device consists of an interchangeable PCR chamber, a temperature control component as well as an optical detection system. The DNA amplification happens on an interchangeable chip with the volumes as low as 1.25 μl , while the heating and cooling rate was as fast as 12.7°C/second ensuring that the total time needed of only 25 min to complete the 35 cycle PCR amplification. An optimized PCR with two-temperature approach for denaturing and annealing (T_d and T_a) of DNA was also formulated with the PCR chip, with which the amplification of male-specific

sex determining region Y (SRY) gene marker by utilizing raw saliva was successfully achieved and the genetic identification was *in-situ* detected right after PCR by the optical detection system.

Keywords Point-of-Care Testing · Molecular diagnostics · Polymerase chain reaction (PCR) · Microfluidic Chip

1 Introduction

Over the past few decades, microfluidic or lab-on-a-chip (LOC) systems have been demonstrated to have great potential to create portable point-of-care (POCT) medical diagnostic devices. Such devices can be designed to obtain and process measurements automatically from small volumes of complex fluids with advanced efficiency and speed (Yager et al. 2006). Among the microfluidic applications on POCT, the development of PCR-based POCT devices has gained much of attention (Daar et al. 2002; Mahalanabis et al. 2010; Sia and Kricka 2008). Such kind of devices can extract the genetic material (the DNA or RNA), amplify by PCR and detect—all in one box, and in very short time duration. The detection of DNA and its variation is critical for many fields, including clinical and veterinary diagnostics, industrial and environmental testing, and forensic science. Disease diagnosis and prognosis are based on effective detection of disease conditions (e.g. cancer), infectious organisms (e.g. HIV) and genetic markers. Diseases caused by infectious bacterial and viral DNA can be detected by PCR. PCR's high sensitivity enables virus detection soon after infection and even before the onset of disease. In most microfluidics applications, the DNA is first purified from tissues or bodily fluids (whole blood, serum, saliva, urine, stool, cerebral spinal fluid, tissues and cells) preparatory to PCR. DNA purification is performed before

Electronic supplementary material The online version of this article (doi:10.1007/s10544-011-9595-6) contains supplementary material, which is available to authorized users.

J. Wu · W. Wen (✉)
Nano Science and Nano Technology program and Physics Department,
The Hong Kong University of Science and Technology,
Clear Water Bay,
Kowloon, Hong Kong
e-mail: phwen@ust.hk

R. Kodzius
KAUST-HKUST Micro/Nanofluidic Joint Laboratory,
The Hong Kong University of Science and Technology,
Clear Water Bay,
Kowloon, Hong Kong

K. Xiao
Department of Biology,
The Hong Kong University of Science and Technology,
Clear Water Bay,
Kowloon, Hong Kong

J. Qin
Dalian Institute of Chemical Physics,
Chinese Academy of Sciences,
457,
Zhongshan Road, 11603, China

loading onto the chip or as an additional step incorporated into microfluidics design (Chen et al. 2007; Lien et al. 2009; Ng et al. 2004). There are some reports of successful amplification directly from blood or saliva (Park et al. 2008). Such non-invasive methods are preferable as they are direct and fast. By careful selection of suitable components and conditions, we succeeded in formulating a simplified and optimized PCR condition for DNA amplification utilizing raw saliva.

The integration of all functions into one chip is not only very difficult technically, but also raises the overall costs of the chip and the assay. At the same time, PCR has a major limitation of risk of cross-contamination. To minimize this risk, PCR chips are always disposable. The disposing of integrated chip leads to a lot of waste in resource though there are some functional parts, such as expensive metals like platinum (Pt) heater and thermal sensor which still can be reusable. Performing PCR in microfluidic chip has advantages such as smaller sample volume along with a higher heat-transfer rate. However, the possible evaporation-induced liquid loss may result in insufficient PCR product for the detection. To avoid it, integrated chips reported so far have used mineral oils (Anderson et al. 2000; Khandurina et al. 2000; Lagally et al. 2000; Lagally et al. 2001; Lee et al. 2004; Waters et al. 1998), tape (Zhao et al. 2003), Bostik's Blu-Tacksilicone (Yeung et al. 2008), rubber gaskets (Yoon et al. 2002), microvalves (Lagally et al. 2001; Lagally et al. 2004; Ramalingam et al. 2009), and long narrow diffusion channels (Wang et al. 2008). All of them need extra materials to provide physical confinement or extra channel structure.

In this work, rather than integrating more functions into one chip, we designed PCR device consisting of a temperature control system, an optical detection system and an interchangeable (disposable or modular) PCR chip, where the PCR chip is independent from the two functional systems. To minimize the evaporation-induced liquid loss, the interchangeable PCR chip was designed to be sealed by the heater directly, eliminating additional manual operations or complicated structures. The heating and cooling rate was as high as 12.7°C/second. As a result, SRY gene was successfully amplified in our chip within 25 min using the optimized condition. Genetic identification was detected right after PCR using raw saliva as template by the optical detection system.

2 Experimental

2.1 Chip design, fabrication and layout

The PCR chip is composed of silicon (double-side polished, <100>) and Pyrex glass layers with thickness of 400 and 500 μm respectively. The PCR chamber on the silicon was formed with dry etching method. Afterward, two holes

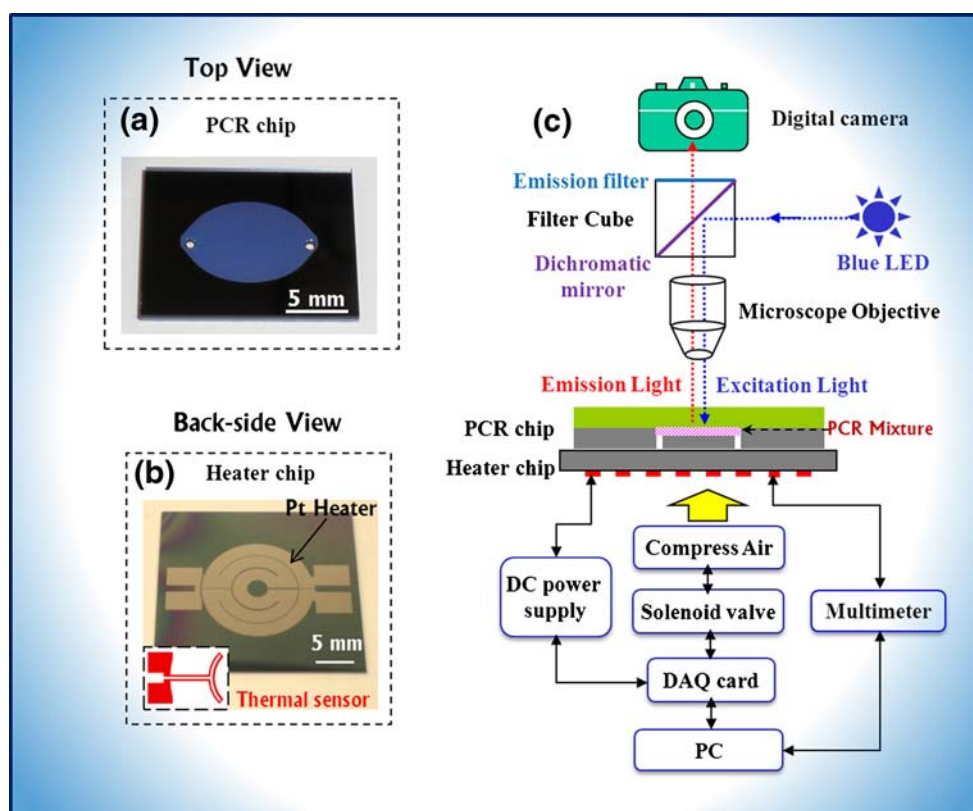
serving as the inlet and outlet of the PCR solution were drilled in the silicon substrate. The silicon substrate was then put into 900°C's furnace to grow 300 nm's silicone dioxide on the surface for passivation and bonded to glass substrate by anodic bonding at last. Then the bonded full wafer was cut into pieces of chip. As can be seen from the PCR chip's upper top view in Fig. 1(a), the silicon and glass substrates were fully bonded together.

Pt thermal sensor and heater on the heater chip was fabricated by lift-off process on a silicon substrate (double-side polished, <100>) coated with 3 μm thermal silicon oxide for electrical insulation. The back-side view of heater chip is shown in Fig. 1(b). The inset is a full view (not to scale) of Pt thermal sensor. The Pt heater was designed to be 2 mm in width to form a low electrical resistance (22 Ω in room temperature) for fast heating. On the contrary, the Pt thermal sensor is narrow and small (20 μm in width), for fast thermal response and has a higher electrical resistance (363 Ω in room temperature) for precise correlation to temperature. An enlarged partial view is shown in Fig. S4A. The heater chip was fixed onto an in-house made holder (Fig. S4B) by a press plate. When performing PCR, the PCR chip was attached tightly on the top-side of heater chip which can be realized by snuggling them each other with two press plates.

2.2 Temperature control

To obtain high-precision temperature control with effective heating and cooling rates, the temperature control system shown in the lower pannel of Fig. 1, custom-designed and constructed in this work, was used. A multimeter (Agilent 34401A, 6 1/2 Digit Multimeter) to measure electrical resistance of thermal sensor, while a solenoid valve (V290, Shinyeong Mechatronics Co., Ltd.) was used to control on-off state of compressed air during cooling process. The heater is controlled by a DC power supply which is connected to a data acquisition card (National Instrument PCI-6259) to obtain the analogue signal used to control the solenoid valve and DC power supply, respectively. A personal computer (PC) with Labview program (National Instruments, Texas, USA) is used for connecting all the other devices and data processing. The resistance of Pt thermal sensor measured by the multimeter is converted to temperature degree under the calibrated resistance-temperature relationship in Labview program. A PID (proportional-integral-derivative) controller in the Labview program used to calculate the output current to the heater based on the error between the set temperature (T_s) and the measured temperature (T_{ms}). If T_{ms} is lower than T_s , an electrical current will be applied to the heater until $T_{ms} = T_s$. For best performance, the PID parameters used in the calculation were tuned in this temperature control system. The PID controller calculation involves three separate

Fig. 1 PCR devices layout. (a). Top view of PCR chip; (b). Back-side view of heater chip; (c). Upper panel is optical detection system. Central panel is chip layout of self-sealed. PCR chip was put on the backside of heater chip after PCR mixture was injected into PCR chamber. Lower panel is temperature control system connected to heater chip



parameters: the proportional, the integral and derivative values, denoted as P, I, and D. In this work, we used manual method to tune these three parameters one by one. To control the reaction time precisely at T_d and T_a , a state machine (Fig. S5A) was set up in Labview program for cycling T_s , so that T_{ms} will follow T_s loop until the state machine finish the set cycles and DNA will be amplified after certain thermal cycles. To obtain a fast cooling rate, the compress air is used to cool down the heater to a certain assigned temperature via a solenoid valve.

2.3 Optical detection

As illustrated in the upper pannel of Fig. 1, the optical detection system consists of a blue LED (MBLED, 625 mW, Thorlabs), a filter cube (U-MWIB2, Olympus), a microscope (Olympus IX-71 Inverted Microscope) with a 4× objective and a digital camera (EOS Rebel T1i, Canon). The blue LED, filter cubes and digital camera were all mounted on the microscope. The filter cube contains a dichromatic mirror (DM505, Olympus) and an emission filter (BA510-IF, Olympus). The dichromatic mirror is positioned in the light path at a 45° angle and selectively reflects wavelengths between 440 and 490 nm, however, transmitting other wavelengths at the same time. The blue excitation given out by the blue LED reaches the dichromatic mirror and is reflected onto PCR mixture

through the glass layer of PCR chip. The SYBR green I (maximum absorption = 498 nm) binds to dsDNA. When excited by the blue light, a green fluorescence emission (maximum emission = 522 nm) passes through the glass layer, the dichromatic mirror and the emission filter and eventually arrives at the digital camera. The emission filter is long pass filter, which allows only light of wavelengths greater than 510 nm to reach the digital camera. The emission filter effectively prevents excitation light wavelengths either reflecting from the PCR chip or successfully traversing the dichromatic mirror from reaching the digital camera.

2.4 PCR components optimization

We chose PCR components and optimized conditions for DNA amplification on the microfluidic chip. Our objective was to have a low T_d along with a small difference between the T_d and T_a . To that end, we took into consideration the PCR components and their concentrations (see supporting information). We tested cytomegalovirus (CMV) primer pairs CMV368F & CMV409R (71 bp) and CMV74F & CMV409R (364 bp) with four different polymerases and their corresponding buffers (Supplemental Figure S2). On bench PCR cycler the SpeedStar performed well both in amplifying shorter (71 bp) and longer (364 bp) DNA fragments under same cycling conditions (extension time

Table 1 Primer sequence and characteristics

DNA source	Region	Primers	Sequence	Length, bp	T _m , °C	GC, %
Saliva	SRY	SRY93F	ATAAGTATCGACCTCGTCGGAAG	23	61.77	47.80
Saliva	SRY	SRY93R	GCACTTCGCTGCAGAGTACCGAAG	24	69.52	58.30
Plasmid vector	CMV	CMV74F	ACGGTAAATGGCCCGCTGGCTGA	24	77.84	62.50
Plasmid vector	CMV	CMV368F	ATGCGGTTTTGGCAGTACATCAATGGGCGT	30	80.29	50.00
Plasmid vector	CMV	CMV409R	GGGTGGAGACTTGAAATCCCCGTGAGTCA	30	78.80	56.67

20 s). For the PCR reactions, we chose primers of 24–30 bases in length (Table 1).

pEGFP-C1 vector (GenBank accession #: U55763; total size: 4.731 kbp) was purchased from Clontech. Primers were selected using FastPCR software (PrimerDigital, Finland) (Kalendar et al. 2009). Size, T_m and GC% values of primers and PCR products were calculated using NetPrimer (Premier Biosoft International, USA).

The PCR consisted of the following components at their final concentrations: 0.75 μM primers (Life Technologies), 3.5 mM MgCl₂ (KapaBiosystems), 0.2 mM dNTP (Takara Bio Inc.), up to 0.2 mM (0.008%) cresol red (Sigma), 1.2 M Betaine (Sigma) and 0.025 U/μl SpeedStar HS (Takara Bio Inc.).

For the purposes of viral sequence detection, we serially diluted plasmid vector so as to have 10 000, 100 000 and 1 million vector molecules in one microliter. We designed primers for the CMV virus and SRY gene sequences (Table 1). Unstimulated whole-saliva samples were collected

by passive drool. One microliter of saliva was used in a 20 μl PCR reaction.

The bench thermocycler employed was MyGenie 96 Gradient Thermal Block (Bioneer Corporation), which uses Peltier elements for heating/cooling and has a ramping rate of 2.5°C per second (maximum).

PCR product detection was achieved by running samples in 3–4% Agarose gel containing SYBR Safe DNA stain (Life Technologies) and by subsequent gel imaging. A DNA ladder (Life Technologies) was applied as a reference in estimating the sizes of DNA fragments. Quantification of band relative intensity was performed by ImageJ version 1.43 software (developed at the National Institutes of Health), subtracting the background and measuring the area of the peak. The obtained value for the band intensity was defined as relative band intensity (RBI). For on-chip detection, SYBR green I (Life Technologies, 10 000x), was diluted to 1x using TE buffer for the final concentration in PCR mixture.

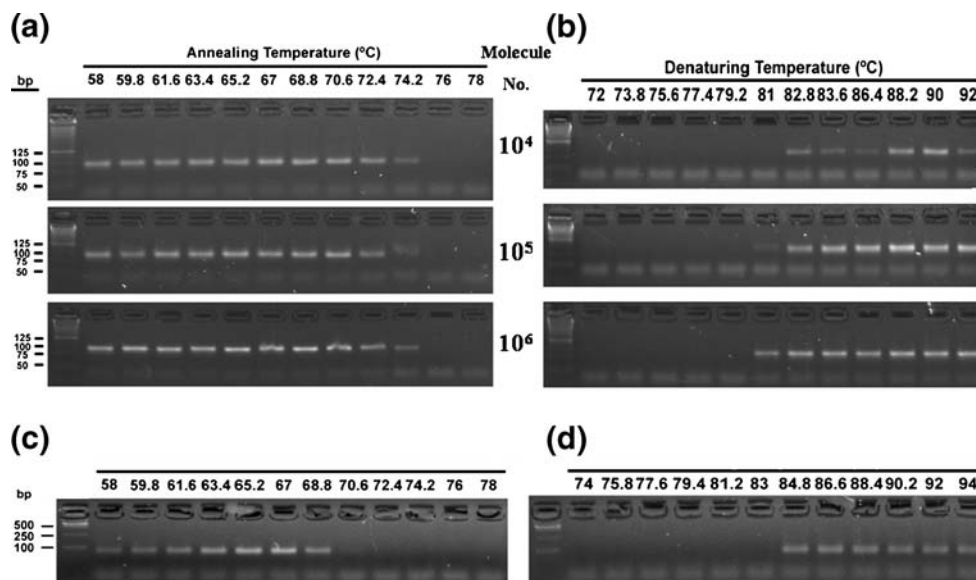


Fig. 2 PCR condition optimizations. A & B. The T_d and T_a optimization using primer pair CMV368F & CMV409R for the 71 bp amplicon. Here the DNA can be amplified from a T_d >81°C with the optimal value of ~90°C. Optimal T_a ranges from <58°C to the highest T_a that can be used in this case, 74.2°C; The T_a (a) and T_d (b) optimization using primer pair SRY93F & SRY93R for the 93 bp

amplicon. PCR amplification from raw saliva is successful with the highest T_a of 68.8°C and minimum T_d of 84.8°C. C & D. The T_a (c) and T_d (d) optimization using primer pairs SRY93F & SRY93R for the 93 bp amplicon. PCR amplification from raw saliva is successful with the highest T_a of 68.8°C and minimum T_d of 84.8°C

Table 2 Oligo pairs and experimental results

Oligo 1	Oligo 2	Product, bp	T _a [min–max]	T _d [min]	Region GC,%
CMV409R	CMV368F	71	71 [<58.0–74.2]	90 [>81.0]	53.5
SRY93F	SRY93R	98	67 [<58.0–68.8]	85 [>84.8]	54.8

3 Results and discussion

3.1 T_d and T_a optimization using viral template DNA

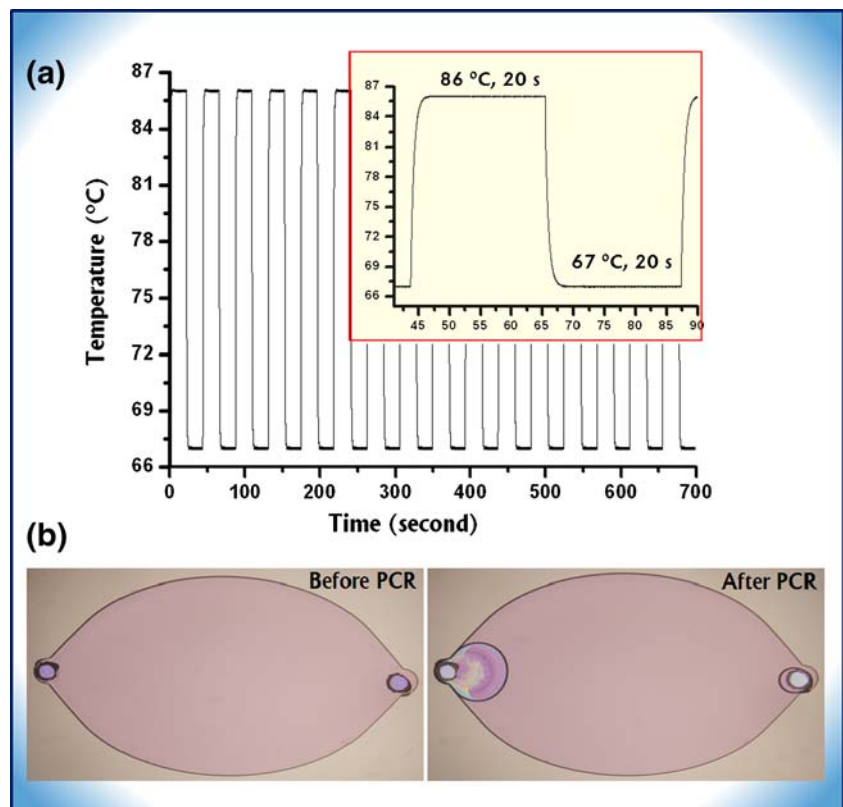
To detect the viral sequence of CMV, we employed a serial dilution of plasmid DNA with concentration of 10^4 , 10^5 and 10^6 molecules in one microliter. Primers for CMV viral sequence were designed (Table 1 and Fig. S1). For the CMV368F & CMV409R primer pair for the 71 bp the T_a was optimized in the PCR using a 58–78°C gradient. The calculated oligo T_m range was 78.80–80.29°C. Experiment was conducted using the SpeedStar HS polymerase. The PCR conditions were 94°C for 20 s, followed by the gradient [58–78] °C for 20 s, and a total of 35 cycles. In the results, we observed that the optimal T_a for the primer pair CMV368F & CMV409R (71 bp) ranged from <58°C to the highest T_a that could be used, 74.2°C (Fig. 2(a) and Table 2).

After we obtained the optimal T_a value, we used the similar approach to determine the optimal T_d. We applied a

72–92°C temperature gradient. Using the primer combination CMV368F & CMV409R (71 bp), the DNA could be amplified from a T_d>81°C with an optimal value of ~90°C (Fig. 2(b) and Table 2). The T_a and T_d can be chosen in such a way that even if the temperature is a few degrees lower or higher (in this example even over 16°C range), the amplification product can still be observed.

We compared the conventional three-temperature PCR with two-temperature PCR used in our experiments. In the results, we could achieve a better control of final product with the two-temperature PCR, whereas some unspecific bands were generated in the three-temperature setup. Similar observations already have been made. (Dodson and Kant 1991) Higher annealing temperature in two-temperature PCR in comparison to three-temperature PCR contributes to the higher specificity. (Weighardt et al. 1993) The developed two-temperature PCR profile, thus, was deemed suitable for amplification of short DNA product, both in microfluidics and bench-thermocycler PCR.

Fig. 3 Thermal cycling performances in chip. (a). 16 thermal cycling result achieved by the temperature system. The inset is one thermal cycling for 86°C and 67°C with time duration of 20 s; (b). Evaporative loss comparison



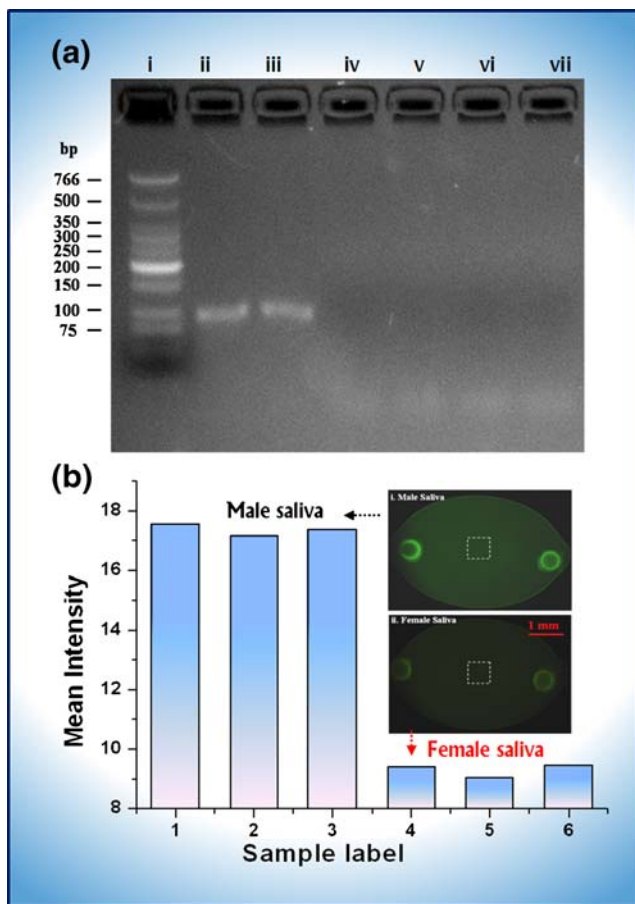


Fig. 4 PCR results in chip. (a). Electrophoresis gel result: i. DNA ladder, ii. male saliva in bench machine, iii. male saliva in chip, iv. female saliva in bench machine, v. female saliva in chip, vi. negative control in bench machine, vii. negative control in chip; (b). The mean fluorescence intensity of PCR results using male (sample 1–3) and female (sample 4–6) saliva as template. i. male saliva, ii. female saliva. The two inset are fluorescence images obtained by the optical detection system after PCR: i. male saliva, ii. female saliva

3.2 PCR using unpurified saliva as DNA source

After initial success in optimizing the T_a and T_d for selected primer pairs, we decided to use the same strategy to optimize the PCR to amplify DNA directly from whole saliva. Saliva is an ideal material for the diagnostics, as it is easy to collect, consists of ~99% water, and contains cells (Dodds et al. 2005). There have been numerous diagnostics tests developed for PCR using saliva as the DNA source, tests both for viral diseases (Blackbourn et al. 1998; Crepin et al. 1998) and for bacterial infections (Eguchi et al. 2003). Here, we chose primer pairs from the SRY gene (GeneBank ID 4507224; Table 1 and Fig. S2). The primers were designed for a final PCR-product size of 93 bp. The T_a was determined by fixing the T_d to 94°C and running the PCR with a 58–78°C annealing gradient. We could observe

bands on the gel even for saliva collected more than a year ago and stored at -20°C . The results indicated the highest T_a of 68.8°C when we could detect PCR products for the 93 bp SRY fragment (Fig. 2(c) and Table 2). The calculated oligo T_m ranged from 61.77 to 69.52°C. To determine the optimal T_d temperature, we used a 74–94°C T_d gradient while keeping the T_a constant at 65°C. In the results, we could see that the minimum T_d for which PCR products could be obtained for the 93 bp SRY fragment was 84.8°C.

The 86°C T_d is an advantageous alternative for chip PCR, as it is much lower than the usual 95°C. A low T_d reduces chip-material interaction with PCR components and imparts the chip with enhanced heat transferability, minimizing the time and energy required to reach the necessary temperature. The difference between the T_d and T_a for the amplification on chip was only 19°C.

3.3 Thermal cycling performance of chip PCR

Not like many other previously reported PCR device, where the PCR chamber and heater were usually integrated into one chip, (Lagally et al. 2001; Lagally et al. 2004; Lee et al. 2004; Yoon et al. 2002; Zhao et al. 2003; Zhong et al. 2009) the heater and the PCR chamber of our PCR device can be easily assembled from individual component which is shown in Fig. 1, therefore, much flexible and changeable as needed. Once the heater chip is fabricated, it can be reused and only need to replace the PCR chamber for different purposes.

Figure 3(a) shows a result of 16 thermal cycles for the ascendant as well as the descendent of temperature between 86°C and 67°C with time duration of 20 s for each. It can be seen from an inset in Fig. 3(a) that very rapid change of temperature can be achieved as fast as 1.5 s. The heating and cooling rate is as high as 12.7°C/s and the accuracy of temperature control is less than $\pm 0.1^\circ\text{C}$.

Since Si has a higher thermal conductivity ($149 \text{ W m}^{-1} \text{ K}^{-1}$) than glass ($1 \text{ W m}^{-1} \text{ K}^{-1}$). The inlet and outlet of the PCR chip were designed in Si layer instead of glass layer and a faster heat exchange (including heating and cooling) can be achieved between Pt heater and PCR mixture. Meanwhile, the inlet and outlet of the PCR chip can be sealed by the backside of heater chip as shown in Fig. 1(c). We call it self-sealed layout since the PCR chip can be sealed without other materials such as mineral oil or other structures. The heater's temperature is always equal to Si layer in the PCR chip, so this design can prevent the leakage and condensation of water vapour on the inlet and outlet of PCR chip. To evaluate evaporative loss of this design, we need to know the volume of PCR mixture before and after PCR. We took two pictures (in Fig. 3(b)) of the PCR mixture in the PCR chamber before and after 35 thermal cycles (86°C for 20 s and 67°C for 20 s). Then we measured the area variation. After testing 10

chips, the evaporative loss was figured out to be only 6% in average. During PCR, very few bubbles were observed due to the uniform thermal distribution (Fig. S6) and low T_a . The evaporation and bubble generation are two common negative effects for temperature controlling. Their minimization in turn will improve the PCR productivity.

3.4 On-site determination of genetic information

We performed an On-Chip PCR using optimized two-temperature cycling process for the primer pair SRY93F & SRY93R, where T_d and T_a are chosen to be respective 86°C and 67°C with duration time of 20 s of each for 35 cycles. PCR chambers used for the experiments here are 50 mm² in area and 100 μm in depth which can contain 5 μl reagents in volume. We injected 5 μl of PCR mixture into the PCR chamber by pipet and run 35 thermal cycles (each cycle is set to 86°C/20 s and 67°C/20 s) using the optimized conditions. To verify the repeatability and specificity of our chip, we have tested it with various saliva sources. The electrophoresis gel result of bench machine and PCR chip is shown in Fig. 4(a). Three PCR were done in three different PCR chips. The 93 bp DNA was successfully amplified both in chip and bench machine and there were no unspecific bands. From intensity of the two bands in lanes ii ($RBI=1.7 \times 10^4$) and iii ($RBI=1.5 \times 10^4$), the amplification efficiency in chip is comparable as in bench machine. As expected no PCR product was observed in PCR using the female saliva due to lack of SRY gene. Negative control result indicates that there is no cross-contamination between the chips. These results indicate that, under optimized PCR conditions by utilizing raw saliva, genetic DNA can be successfully amplified in our PCR chip.

In order to detect genetic information *on-site*, we designed an optical detection system shown in Fig. 1(c), which can detect dsDNA by the fluorescence intensity. For optical detection in chip, we reduced the volume to 1.25 μl with different PCR chamber where the height and area were reduced to 50 μm and 25 mm², respectively. We have tested 6 saliva samples collected from 3 male (Sample 1–3) and 3 female (Sample 4–6) volunteers. After PCR was performed in chip, we took the fluorescence image in a dark-room and exposure time was set to ¼ second. We used ImageJ software to measure the mean fluorescence intensity (MFI) of 50 pixels×50 pixels (white dash square in the centre of PCR chamber in Fig. 4(b)). The results are plotted in Fig. 4(b). Two insets in Fig. 4(b) show the fluorescence images tested with male and female saliva, respectively. We can see clearly that there is a difference in fluorescence intensity between two images: the male one (MFI=17.7) is brighter than the female one (MFI=9.0) due to the amplified target DNA.

4 Conclusions

Successful DNA amplification and detection on chip depends on the optimization of many parameters including primers design, T_a and T_d . We demonstrate that for PCR primer pair and two-temperature PCR, T_a can be optimized first, following with T_d optimization. Si and glass in PCR chip can be easily replaced to cheaper materials such as low cost polymer since the PCR chip is independent from the two functional systems. The PCR chip was directly combined by the heater chip avoiding the unnecessary complicated structure. This self-sealed design has not only a very high efficiency to prevent evaporation loss of reagents but also easy to handle. By using such design, the faster PCR with less than 25 min can be achieved. On-site testing for gene identification with raw saliva has been realized by fluorescence methodology which provides a promising prototype for developing PCR-based molecular POCT handheld device.

Acknowledgements The authors acknowledge the financial support provided by the Hong Kong Research Grants Council Grant No. HKUST 603608. This publication is based on work partially supported by Award No. SA-C0040/UK-C0016 made by King Abdullah University of Science and Technology (KAUST).

References

- R.C. Anderson, X. Su, G.J. Bogdan, J. Fenton, *Nucleic Acids Res.* **28**, (2000)
- D.J. Blackburn, E.T. Lennette, J. Ambroziak, D.V. Mourich, J.A. Levy, *J. Infect. Dis.* **177**, 213 (1998)
- Z. Chen, M.G. Mauk, J. Wang, W.R. Abrams, P.L.A.M. Corstjens, R. S. Niedbala, D. Malamud, H.H. Bau, *Ann New York Acad Sci* **1098**, 429 (2007)
- P. Crepin, L. Audry, Y. Rotivel, A. Gacoin, C. Caroff, H. Bourhy, *J. Clin. Microbiol.* **36**, 1117 (1998)
- A.S. Daar, H. Thorsteinsdóttir, D.K. Martin, A.C. Smith, S. Nast, P.A. Singer, *Nat. Genet* **32**, 229 (2002)
- M.W.J. Dodds, D.A. Johnson, C. Yeh, *J. Dent* **33**, 223 (2005)
- L.A. Dodson, J.A. Kant, *Mol. Cell. Probes* **5**, 21 (1991)
- J. Eguchi, K. Ishihara, A. Watanabe, Y. Fukumoto, K. Okuda, *Oral Microbiol. Immunol.* **18**, 156 (2003)
- R. Kalendar, D. Lee, A.H. Schulman, *Genes Genomes Genomics* **3**, 1 (2009)
- J. Khandurina, T.E. McKnight, S.C. Jacobson, L.C. Waters, R.S. Foote, J.M. Ramsey, *Anal. Chem.* **72**, 2995 (2000)
- E.T. Lagally, C.A. Emrich, R.A. Mathies, *Lab Chip* **1**, 102 (2001)
- E.T. Lagally, P.C. Simpson, R.A. Mathies, *Sens Actuators B Chem* **63**, 138 (2000)
- E.T. Lagally, J.R. Scherer, R.G. Blazej, N.M. Toriello, B.A. Diep, M. Ramchandani, G.F. Sensabaugh, L.W. Riley, R.A. Mathies, *Anal. Chem.* **76**, 3162 (2004)
- D. Lee, S.H. Park, H. Yang, K. Chung, T.H. Yoon, S. Kim, K. Kim, Y. T. Kim, *Lab Chip* **4**, 401 (2004)
- K. Lien, C. Liu, P. Kuo, G. Lee, *Anal. Chem* **81**, 4502 (2009)
- M. Mahalanabis, J. Do, H. Almuayad, J.Y. Zhang, C.M. Klapperich, *Biomed. Microdevices* **12**, 353 (2010)

- D.P.K. Ng, D. Koh, S.G.L. Choo, V. Ng, Q. Fu, *Clin. Chim. Acta* **343**, 191 (2004)
- S.J. Park, J.Y. Kim, Y.G. Yang, S.H. Lee, *J. Forensic Sci.* **53**, 335 (2008)
- N. Ramalingam, H. Liu, C. Dai, Y. Jiang, H. Wang, Q. Wang, K.M. Hui, H. Gong, *Biomed. Microdevices* **11**, 1007 (2009)
- S.K. Sia, L.J. Kricka, *Lab Chip* **8**, 1982 (2008)
- F. Wang, M. Yang, M.A. Burns, *Lab Chip* **8**, 88 (2008)
- L.C. Waters, S.C. Jacobson, N. Kroutchinina, J. Khandurina, R.S. Foote, J.M. Ramsey, *Anal. Chem.* **70**, 158 (1998)
- F. Weighardt, G. Biamonti, S. Riva, *Genome Res.* **3**, 77 (1993)
- P. Yager, T. Edwards, E. Fu, K. Helton, K. Nelson, M.R. Tam, B.H. Weigl, *Nature* **442**, 412 (2006)
- S.S.W. Yeung, T.M.H. Lee, I. Hsing, *Anal. Chem.* **80**, 363 (2008)
- D.S. Yoon, Y. Lee, Y. Lee, H.J. Cho, S.W. Sung, K.W. Oh, J. Cha, G. Lim, *J. Micromech. Microeng.* **12**, 813 (2002)
- Z. Zhao, Z. Cui, D. Cui, S. Xia, *Sens. Actuat. A Phys.* **108**, 162 (2003)
- R. Zhong, X. Pan, L. Jiang, Z. Dai, J. Qin, B. Lin, *Electrophoresis* **30**, 1297 (2009)